J. Physiol. (1985), **366**, *pp.* 177–195
With 1 plate and 8 text-figures
Printed in Great Britain

ELECTRIC CURRENT FLOW IN CELL PAIRS ISOLATED FROM ADULT RAT HEARTS

BY P. METZGER AND R. WEINGART

From the Department of Physiology, University of Berne, Bühlplatz 5, CH-3012 Berne, Switzerland

(*Received 23 January 1985*)

SUMMARY

1. Cell pairs were isolated from ventricles of adult rat hearts so as to study cell-to-cell coupling.

2. Both cells of each pair were impaled with micro-electrodes connected to balanced bridge circuits. Rectangular current pulses were passed and the resulting voltage deflexions monitored.

3. The data were analysed in terms of a delta configuration of three resistive elements, the resistances of the non-junctional membrane of cell 1 and cell 2 ($r_{m,1}$ and $r_{m,2}$), and the resistance of the nexal membrane (r_n).

4. The nexal membrane resistance was found to be insensitive to voltage gradients across the non-junctional membrane (range examined: -70 to -10 mV) and direction of current flow.

5. The mean value of r_n was 2·12 MΩ ($[K^+]_o = 12$ mM). Taking into account morphological parameters, this corresponds to a specific nexal membrane resistance (R_n) of 0·1 Ω cm².

6. Spontaneous uncoupling in which one cell remained polarized while the other one depolarized was never observed.

7. The current–voltage relationship of the non-junctional membrane was found to be bell-shaped. The specific resistance (R_m) at the resting membrane potential (~ -50 mV) was 3·2 kΩ cm² ($[K^+]_o = 12$ mM).

8. Comparative studies performed on single cells revealed a similar relationship R_m *versus* V_m. R_m at the resting membrane potential ($V_m \sim -50$ mV) was 2·5 kΩ cm² ($[K^+]_o = 12$ mM).

9. The specific capacitance of the non-junctional membrane (C_m) was determined from experiments on single cells. C_m was found to be independent of V_m (voltage range: -80 to 0 mV). The mean value of C_m was 1·66 μF/cm² ($[K^+]_o = 12$ mM).

10. For comparison, experiments on cell pairs and single cells were also carried out with $[K^+]_o = 4$ mM. The values obtained for R_n, R_m and C_m did not deviate significantly from those found with $[K^+]_o = 12$ mM.

INTRODUCTION

Hodgkin & Rushton (1946) were the first investigators who successfully applied the linear core conductor concept to a single cell, the crustacean nerve fibre. The model assumed a structure consisting of a resistive core (the cytoplasm) surrounded by an imperfect frequency-dependent insulator (the cell membrane), which allowed leakage of current to ground. Shortly thereafter, Weidmann (1952) demonstrated that the equations derived from this model also adequately described the passive electrical behaviour of a syncytial tissue, the cardiac Purkinje fibre. Since then the linear cable analysis has been used by a number of investigators to obtain quantitative information concerning the passive electrical properties of cardiac tissue. Studies have been performed on both working myocardium and specialized tissues isolated from different species (for references, see Fozzard, 1979; Weingart 1981; Berkenblit, Boschkova, Bojzowa, Mittelman, Potapowa, Tschajlchjan & Scharoskaja, 1981; De Mello, 1982). From these investigations, it has been elucidated that cardiac cells are connected via low resistance elements (r_n or r_{nexus}), which also may be in parallel with a capacitive element (c_n or c_{nexus}).

Despite its great success this multicellular approach is limited by tissue geometry and methodological restrictions. The assumptions underlying cable analysis require a uniform cross-sectional diameter and parallel flow of current intracellularly and extracellularly, at all distances from the current source (Hodgkin & Rushton, 1946). Furthermore, intracellular and extracellular resistances per unit length have been assumed to be constant. It would seem that the complex three-dimensional cellular network of all cardiac tissue may preclude some of the conditions necessary for a precise analysis (e.g. Eisenberg & Cohen, 1983; Levis, Mathias & Eisenberg, 1983). Furthermore, most investigators simply neglected the contribution of extracellular resistivity. This simplification may be tolerable when considering a single cell but not for a multicellular preparation with a restricted extracellular space (Mathias, 1983). In addition, some methods require precise knowledge of the ratio of intra- *versus* extracellular volume, which could introduce additional uncertainties. In the case of a point source of current, three-dimensional current spread in the vicinity of the current source also may have to be considered (Eisenberg & Johnson, 1970; Pressler, 1984).

Over the last few years enzymatic procedures have been developed for isolating cardiac cells from adult hearts (e.g. Powell, Terrar & Twist, 1980; Fabiato, 1981; Isenberg & Klöckner, 1982*a*). In addition to a large number of single cells, these techniques yield a sizeable fraction of cell pairs and larger aggregates. Such cell pairs may represent a suitable preparation for studying the electrical properties of both junctional (nexal) and non-junctional (sarcolemmal) membranes. This new approach seems promising because it enables quantitative study of the electrical properties of a single connexion between two individual cells. Thus, it would help to overcome some of the difficulties which to date have hampered quantitative analysis of nexal properties *in situ*. As a matter of fact, Kameyama (1983) recently reported successful measurements performed on cell pairs isolated from guinea-pig heart.

In this study we have attempted to quantify the passive electrical properties of isolated myocytes and myocyte pairs utilizing conventional micro-electrode tech-

niques. A bridge circuit was employed to inject constant current pulses and to measure the resulting voltage displacements. Quantitative assessments were obtained for both the non-junctional membrane resistance and the junctional membrane resistance. In addition, the dependence of both membrane resistances on the non-junctional membrane potential was examined. For comparison, these measurements were performed in the presence of two different external K^+ concentrations, i.e. $[K^+]_o$ of 4 and 12 mM.

A preliminary report of some of the experiments has been published previously (Metzger & Weingart, 1983).

METHODS

Cell preparation

Sprague–Dawley rats, approximately 8 weeks old and 250 g in weight, were anticoagulated with heparin (intraperitoneally, 1000 units), anaesthetized with ether, stunned by a blow to the neck and the hearts quickly removed. The enzymatic procedure for isolation of the ventricular cells was adapted from the method of Powell *et al.* (1980). The hearts were cannulated for retrograde perfusion through the aorta and pre-perfused for 10–15 min at room temperature with Krebs–Ringer solution (A; the composition of this solution and others is given below) containing heparin (5000 u./l) and insulin (4 u./l). This procedure allowed the hearts to recover from the trauma of removal as judged by the spontaneous rhythm and contractility. The hearts then were transferred to a perfusion apparatus similar to the one described by Powell *et al.* (1980, Fig. 1). The subsequent steps were performed at 37 °C in the following sequence: 2 min of perfusion with solution B; 2 min of perfusion with solution C; 16–18 min of perfusion with solution C (50 ml, recirculated) to which were added 6250 u. collagenase, 50 mg bovine albumin (Sigma), and 1·25 μmol $CaCl_2$ (25 μM). The coronary flow rate was adjusted to approximately 1 drop/s.

At the end of the above perfusion procedure, the ventricles were minced (approximately 1–2 mm thick pieces) using a manual chopping device. Subsequently, the tissue pieces were incubated for 6 min in solution C (20 ml) to which were added 2500 u. collagenase, 20 mg bovine albumin (Sigma), and 0·5 μmol $CaCl_2$ (25 μM). The incubation mix was agitated gently with a Pasteur pipette. The resulting cell suspension was filtered through nylon gauze (width of mesh: 250 μm), centrifuged for 1 min at approximately 20 *g* and the cell pellets resuspended. This filtration and resuspension procedure was performed four times (1)–(4). The following resuspension media were used each time: (1) solution B (20 ml) to which was added 0·5 μmol $CaCl_2$; (2) and (3) solution B (40 ml) to which were added 1600 mg bovine albumin (Miles), and 1 μmol $CaCl_2$ (25 μM); (4) solution B (20 ml) to which was added 10 μmol $CaCl_2$ (0·5 mM). The resulting cells were stored in solution B in which the $CaCl_2$ concentration was increased gradually to 1·8 mM. With this procedure a variable yield of rod-shaped cells was obtained that ranged from 10 to 60% (see Pl. 1). The fraction of cell pairs ranged from 16 to 28% of the intact cells. No attempt was made to alter the isolation procedure to maximize the percentage of cell pairs.

The normal Krebs–Ringer solution (A) contained (mM): NaCl, 140; KCl, 4; $CaCl_2$, 1·8; $MgCl_2$, 1; HEPES, 5 (pH 7·4); glucose, 5. The experiments were performed using either this solution or one with 12 mM-KCl (NaCl equivalently reduced). The cell preparation required the following basic solutions: solution B: normal Krebs–Ringer solution with no added $CaCl_2$. A free Ca^{2+} concentration of approximately 20 μM was found for this solution when measured with a Ca^{2+}-selective macro-electrode (IS 561-Ca, Philips, Zürich, Switzerland). Solution C (mM): potassium glutamate, 124; NaCl, 20; $MgCl_2$, 1; HEPES, 5 (pH 7·4); glucose, 5. All solutions were gassed with 100% oxygen. The following substances were used: bacterial collagenase type I, code CLS (4194, Worthington, Freehold, NJ, U.S.A.); bovine albumin, essentially fatty acid-free (A 6003, Sigma, Taufkirchen, West Germany); bovine albumin fraction V (81–066, Miles, Cavenago Brianza, Italy).

All glassware in contact with cells was siliconized in an oven at 200 °C using the compound TMSDMA (Fluka, Buchs, Switzerland). For description of the procedure, see Hess, Metzger & Weingart (1982).

Electrophysiology

The experimental recording chamber consisted of a Perspex frame with an attached glass bottom. This was mounted on the stage of an inverted phase-contrast microscope (model Diavert, Leitz, Wetzlar, West Germany). During an experiment, 1 ml saline solution was added to the chamber and the bath connected to ground (Ag–AgCl pellet) via an Agar bridge containing 3 M-KCl. A few drops of the cell suspension then were added and 5 min allowed for the cells to settle to the bottom of the chamber. The cell suspension was replaced approximately every hour. In the course of an electrophysiological experiment, the cells were visualized using an over-all magnification of 320 times (occular: ×10; objective: ×32).

Transmembrane potentials were recorded from single cells or cell pairs using conventional micro-electrodes. When filled with 3 M-KCl, 20 mM-HEPES (pH adjusted to 7·0), and 5 mM-EGTA, d.c. tip resistance measured 30–50 MΩ. The electrodes were placed in standard Ag–AgCl electrode holders (EH-R, WP Instruments, New Haven, CT, U.S.A.) containing electrode-filling solution and

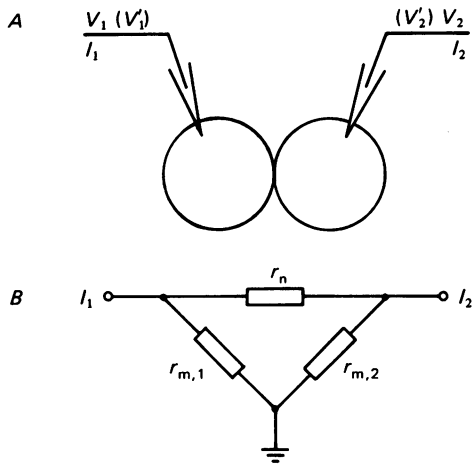

Fig. 1. *A*, diagram of the electrode arrangement for determination of passive electrical properties of a cell pair. Each cell was impaled with a micro-electrode to pass current (I_1 or I_2) and monitor the resulting voltage deflexions (V_1 and V_2', or V_2 and V_1', respectively). *B*, equivalent electric circuit assumed for analysis of the resistive elements: r_1 and r_2 represent the non-junctional membrane resistances of cell 1 and cell 2, and r_n the resistance of the nexal membrane.

connected to unity-gain electrometers (model M 701 and M 707, WP Instruments). The leakage current of the electrometers was regularly adjusted to values less than 5 pA. Current was applied intracellularly via the recording electrode. The voltage drop across the micro-electrode resistance resulting from current flow was cancelled by balancing an active bridge circuit incorporated in the electrometer. This adjustment was performed prior to an impalement and re-checked after electrode withdrawal. Only those experiments were accepted for further analysis in which there was no detectable change. Current was measured directly from the monitor output of the instrument. Duration and frequency of the current pulses were controlled with a digital pulse generator (series 1800, WP Instruments). Polarity and intensity of the current pulses were selected using a voltage divider triggered by the pulse generator. The current and voltage signals were displayed on a storage oscilloscope (series 5113, Tektronix, Beaverton, OR, U.S.A.) and recorded on a four-channel chart recorder (Brush 2400, Gould, Cleveland, OH, U.S.A.).

The input stages of the electrometers and the electrode holders were mounted on hydraulic micro-manipulators (model MO 102, Narashige Scientific Laboratory, Tokyo, Japan). The drive units themselves were mounted on manipulators for coarse movements (model MP 2, Prior, Bishop's Stortford, U.K.). The experimental table damped room vibrations via an air-cushion arrangement.

The input resistance of single cells was determined simply from the slope of the membrane potential displacement–injected current relation (dV/dI). The model used to analyse the cell pair data is illustrated in Fig. 1, in which *A* shows the experimental arrangement and *B* the simplest equivalent circuit. This circuit implies that current flows across three resistive elements arranged in a delta configuration: $r_{m,1}$ and $r_{m,2}$, the non-junctional membrane resistances of cell 1 and cell 2, and r_n, the resistance of the nexal membrane connecting the two cells. The model assumes that current flows via either of two pathways: (1) directly through the non-junctional membrane of the injected cell, or (2) through r_n into the follower cell. In addition, the cytoplasmic resistance is lumped with r_n, and the resistance of the extracellular solution neglected. Employing Kirchhoff's laws, the following equations can be derived from the equivalent circuit (Watanabe & Grundfest, 1961; Bennett, 1966; Metzger & Weingart, 1984):

$$\frac{dV_1}{dI_1} = \frac{r_{m,1}(r_{m,2}+r_n)}{r_{m,1}+r_{m,2}+r_n}, \tag{1}$$

$$\frac{dV_2'}{dV_1} = \frac{r_{m,2}}{r_{m,2}+r_n}. \tag{2}$$

The *input resistance* (eqn. (1)) is defined as the slope of the voltage–current relation when the voltage deflexion is measured in the injected cell. The *coupling coefficient* (eqn. (2)) is defined as the ratio of voltage change in the follower cell over voltage change in the injected cell. These two equations apply to the case of current injection into cell 1; an analogous pair of equations can be obtained for the case of current application to cell 2. With these four equations four separate measurements can be made leading to an evaluation of the three resistive elements of the equivalent circuit.

At the beginning of each experiment the cellular dimensions were measured by means of a micrometer eyepiece in order to express the data in specific terms.

RESULTS

Cell pairs

Intrinsic electrical activity. In intact tissue, cardiac cells are not arranged in register (see e.g. Sommer & Johnson, 1979, fig. 5). Therefore, cell pairs exist in various configurations in a cell suspension. Two-cell preparations attached end-to-end were observed only rarely. In most cases, individual cells were arranged side-to-side with various degrees of overlap. Presumably, this configuration is more mechanically stable in a suspension and hence this was the type of preparation used in our study (see Pl. 1*B*).

Fig. 2 illustrates examples of intrinsic electrical activity observed in ventricular two-cell preparations. Each cell of a cell pair was impaled with a micro-electrode. The signals in the first and second row represent the electrical activity recorded from cell 1 ($V_{m,1}$) and cell 2 ($V_{m,2}$), respectively. The traces in the third row show the voltage difference signal between cell 1 and cell 2 ($V_{m,1} - V_{m,2}$). Fig. 2*A* represents a case of a cell pair that was spontaneously active in Krebs–Ringer solution containing 12 mM-K^+. Starting from a maximal diastolic potential of −47 mV, the cells developed spontaneous action potentials at a frequency of 1·2 Hz. As indicated by the relatively flat difference signal (bottom trace), the action potentials were virtually superimposable. No phase shift was obvious at the time resolution examined.

Fig. 2*B* shows the electrical activity of a partially depolarized preparation exposed to a saline containing 4 mM-K^+. Both cells exhibited spontaneous low voltage oscillations similar to those described in intact cardiac tissue (for references, see Tsien, Kass & Weingart, 1979). The oscillations were slightly irregular both in frequency

(1·1–1·4 Hz) and amplitude (voltage range from −31 to −25 mV). The individual signals were superimposable and without indication of a delay as indicated by the smooth voltage difference trace, $V_{m,1} - V_{m,2}$. Fig. 2*C* shows records of a preparation bathed in Krebs–Ringer solution containing 4 mM-K^+. A small rectangular current pulse of 200 ms duration (fourth row) was applied intracellularly via the electrode in cell 2. This produced hyperpolarizing voltage deflexions in cells 1 and 2 changing V_m from −65 to −75 mV approximately. Upon pulse termination, both cells

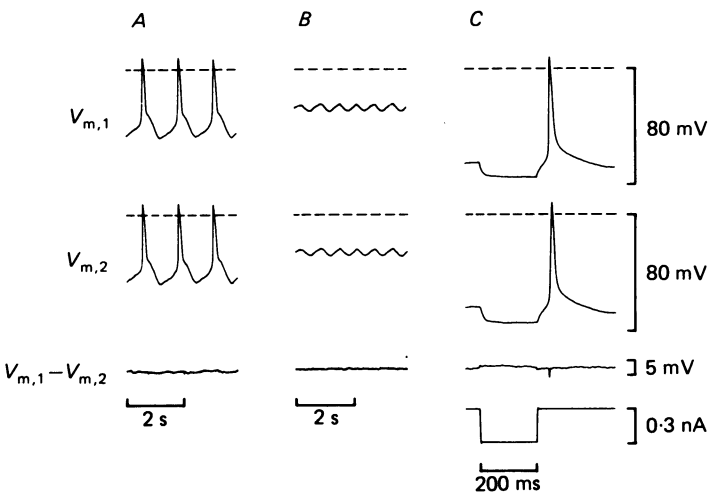

Fig. 2. Intrinsic electrical activity recorded from functionally coupled cell pairs. First and second row: transmembrane potential of cell 1 ($V_{m,1}$) and cell 2 ($V_{m,2}$), respectively; third row: potential difference between cell 1 and cell 2 ($V_{m,1} - V_{m,2}$); fourth row: current intensity. *A*, spontaneous action potentials, $[K^+]_o = 12$ mM; preparation M 89a. *B*, spontaneous low voltage oscillations, $[K^+]_o = 4$ mM; preparation M 79a. *C*, hyperpolarizing electrotonic responses induced by injecting current into cell 2, followed by anodal break responses, $[K^+]_o = 4$ mM; preparation M 92a. Note the increased amplification in the third row and expanded time base in *C*.

responded with an action potential. There was a short spike on the differential record during the upstroke but no further deflexions during the action potential. To this degree of resolution there was no time lag between the action potentials. Nevertheless, it is tempting to assume that the injected cell (cell 2) was the leading cell whereas the other one was the follower cell. During application of a constant current, the voltage difference was positive, signalling a larger voltage deflexion evoked in cell 2 than in cell 1. This is supportive evidence for the existence of a resistive element between cells of a cell pair.

The superimposable action potentials and lack of a delay of the intrinsic electrical signals recorded from individual cells of a cell pair suggest functional coupling between the cells.

Square-pulse analysis. Fig. 3 illustrates an experiment in which the passive electrical properties of a cell pair were investigated using pulses of direct current. In Fig. 3*A*, a small hyperpolarizing current pulse of 200 ms duration (I_1, not shown, but identical to I_2 given in *B*) was injected into cell 1 and the resulting membrane voltage deflexions measured in cell 1 (V_1) and cell 2 (V_2'). Fig. 3*B* shows the corresponding

records upon application of an identical current pulse to cell 2 (I_2). This gave rise to the electrotonic responses V_2 in cell 2 and V_1' in cell 1. In both cases the voltage response in the injected cell was slightly larger than that in the follower cell. The magnitude of the voltage drop across the nexal membrane can be visualized more readily from the voltage difference signals $V_1 - V_2'$ (Fig. 3*A*) and $V_1' - V_2$ (Fig. 3*B*). There was a consistent degree of attenuation of the voltage response when current was applied separately to either side of the nexal junction. This finding suggested that current flows across the nexus equally well in both directions.

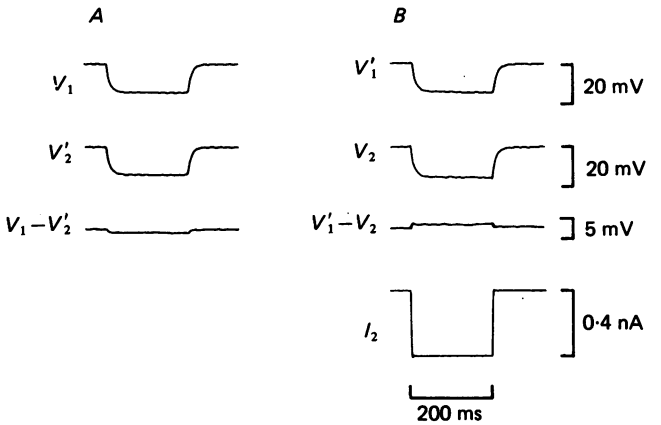

Fig. 3. Current flow in a cardiac cell pair. First and second row: voltage deflexions evoked in cell 1 (V_1, V_1') and in cell 2 (V_2, V_2'); third row: voltage difference between cell 1 and cell 2; fourth row: intensity of intracellularly injected current. Note the expanded voltage amplification in the third row. A hyperpolarizing current pulse of 388 pA was injected alternatively into cell 1 or cell 2 giving rise to the voltage deflexions displayed in *A* and *B*, respectively. Analysis for this data revealed the following resistance values: $r_1 = 75{\cdot}5$ MΩ, $r_2 = 67{\cdot}0$ MΩ, $r_n = 4{\cdot}2$ MΩ. The apparent sarcolemmal area of cell 1 and cell 2 was 8800 μm^2 and 9700 μm^2, respectively. Hence, the specific membrane resistances R_1 and R_2 were calculated to be 6645 Ω cm² and 6500 Ω cm². $[K^+]_o = 12$ mM; $V_m = -35$ mV. Preparation M 64.

Similar measurements were performed over a broad range of membrane potentials. Square current pulses of test current were superimposed at a frequency of 0·5 Hz on holding currents of varying amplitude and polarity. The intensity of the test current pulses was adjusted so that the voltage deflexions would not exceed 15–20 mV, thus minimizing problems due to the nonlinearity of the non-junctional membrane resistance.

The experimental results were analysed for $r_{m,1}$, $r_{m,2}$, and r_n in terms of the equivalent circuit described in Fig. 1. In order to compute the specific resistance of the non-junctional membranes, $R_{m,1}$ and $R_{m,2}$, the mean cellular length and diameter were measured with a micrometer eyepiece prior to each experiment. Each cardiac cell was assumed to be adequately described by a circular cylinder having a smooth surface. An average value of R_m for each cell pair then was calculated from the corresponding individual values of $R_{m,1}$ and $R_{m,2}$. The resistance of the nexal membrane was expressed both in non-specific (r_n) and specific terms (R_n), the latter

requiring knowledge of the surface area of nexal membrane connecting two cells. In this regard, we initiated quantitative studies of the nexal membrane of myocyte pairs using thin sections processed for transmission electron microscopy (P. Gehr & R. Weingart, unpublished). Unfortunately, to date these studies have been unsuccessful, presumably because many cell pairs lose their intercellular connexions during the processing procedure. As an alternative, we resorted to previous stereological measurements on intact rat ventricular muscle reported by Stewart & Page (1978). Their data enable calculation of the nexal membrane area of a single cell in its three-dimensional context:

$$S_n \text{ (single cell)} = (S_n/V_{cell})\, L_{cell}\, l_{sarc}\, (D_{std}/2)^2 \pi, \tag{3}$$

where S_n/V_{cell} is the area of nexal membrane per unit cell volume; L_{cell} is the cell length in sarcomeres; l_{sarc} is the sarcomere length; D_{std} is the equivalent cell diameter. Considering only those measurements from rats similar in body weight to the animals used in our study (above 200 g), S_n (single cell) was determined to be 66·6 μm^2. The nexal membrane area connecting the two cells of a cell pair then was obtained from the following equations (P. Gehr & L. Cruze-Orive, personal communication):

$$S_n \text{ (cell pair)} = S_n \text{ (single cell)}/f, \tag{4}$$

$$f = 2x + 2, \tag{5}$$

where x is a neighbourhood parameter representing the number of cells surrounding a given cell in a given perpendicular cross-section. Examination of randomly selected cross-sections of rat ventricular muscle under the light microscope (magnification: ×400) revealed x to be $5{\cdot}45 \pm 0{\cdot}08$ (mean ± S.E. of mean, $n = 172$) (P. Gehr, unpublished). Therefore, S_n (cell pair) was calculated as 5·16 μm^2.

A series of electrical experiments was performed in Krebs–Ringer solution containing 12 mM-K^+. Fifteen cell pairs were studied successfully and the results plotted as histograms, collecting V_m data in sample bins of 10 mV size.

Fig. 4*A* illustrates the relationship between the specific resistance of the non-junctional membrane (R_m) and the sarcolemmal membrane potential at which the measurements were performed (V_m). The relationship appears to be curvilinear with a maximum R_m of 9610 Ω cm² at −20 mV and a minimum R_m of 2630 Ω cm² at $V_m = -60$ mV, the most negative potential at which reliable measurements could be obtained. Fig. 4*B* illustrates the relationship between junctional membrane resistance (r_n, left-hand ordinate; R_n, right-hand ordinate) and V_m. Considerable scatter of the data was observed with mean r_n values ranging from $1{\cdot}33 \pm 0{\cdot}33$ MΩ ($n = 29$) at a V_m of −50 mV, to $2{\cdot}68 \pm 0{\cdot}51$ MΩ ($n = 23$) at a V_m of −40 mV. Corresponding values of R_n were 0·07 Ω cm² and 0·14 Ω cm² respectively. Statistical analysis revealed no significant correlation between the nexal membrane resistance and V_m ($2\alpha \gg 0{\cdot}1$; correlation coefficient $r = 0{\cdot}084$). The over-all mean r_n was $2{\cdot}12 \pm 0{\cdot}20$ MΩ ($n = 114$) and 0·10 Ω cm² for R_n.

An independent set of experiments was undertaken at a lower $[K^+]_o$ of 4 mM. Fig. 5 summarizes the results gathered from eighteen cell pairs. Fig. 5*A* shows the histogram of the relationship between R_m and V_m. The bell-shaped function exhibited a maximum of 9640 Ω cm² at a V_m of −30 mV, and a minimum of 4360 Ω cm² at the

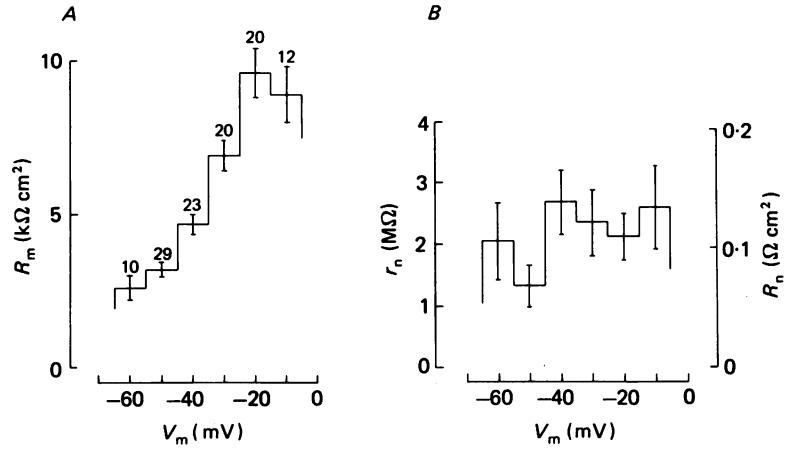

Fig. 4. Passive electrical properties determined from cell pairs exposed to Tyrode solution containing 12 mM-K^+. The specific resistance of the non-junctional membrane (sarcolemmal membrane) R_m (*A*) and the junctional membrane (nexal membrane) R_n (*B*) were plotted as a function of the potential difference across the non-junctional membrane, V_m. The collected data from fifteen cell pairs were analysed, sampled in V_m bins of 10 mV, and plotted as histograms. The bars represent the mean ± 1 S.E. of mean and the accompanying numbers relate to the number of individual observations. Further details concerning the analysis are given in the text.

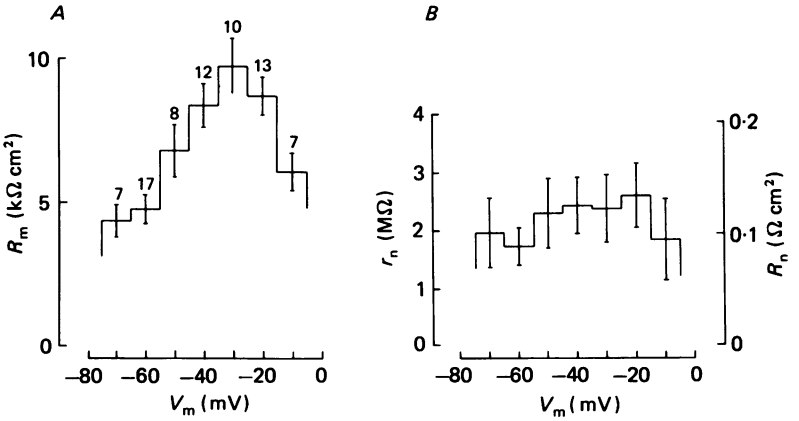

Fig. 5. Passive electrical properties determined from cell pairs immersed in Tyrode solution containing 4 mM-K^+. Format and nomenclature are the same as in Fig. 4. The data summarize the results from eighteen cell pairs.

most negative potential examined, i.e. $V_m = -70$ mV. Fig. 5*B* displays the relationship between r_n and R_n *versus* V_m. Again, there was a substantial variation in the nexal membrane resistance. The smallest mean value of r_n was 1·72 MΩ at $V_m = -60$ mV, and the largest was 2·62 MΩ at $V_m = -20$ mV, corresponding to R_n values of 0·09 Ω cm² and 0·14 Ω cm², respectively. There was no statistically significant correlation between the nexal membrane resistance and V_m ($2\alpha \gg 0{\cdot}1$; correlation coefficient $r = 0{\cdot}091$). From the total number of determinations ($n = 74$), the following mean values were calculated: $r_n = 2{\cdot}27 \pm 0{\cdot}19$ MΩ; $R_n = 0{\cdot}12$ Ω cm².

At this juncture a comment is appropriate regarding the selection of data for analysis. A large number of other experiments on cell pairs also were performed. However, many experiments had to be discarded either because the voltage difference was inconsistent with the assumed direction of current flow, or the differential records were too small to allow reliable analysis. It is possible in these cases that one of the electrodes' resistance altered during the experiment, or that the cells simply were too tightly coupled to permit accurate measurements using this technique. Furthermore, only those experiments were included in which resistance measurements could be carried out successfully for a minimum of three different V_m levels.

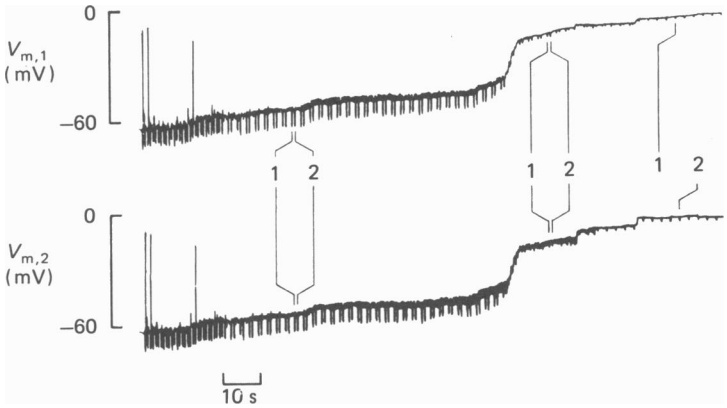

Fig. 6. Terminal behaviour of a cell pair. Progressive depolarization of V_m in cell 1 (upper trace) and cell 2 (lower trace) was associated with a decrease of R_m in both cells. This was suggested by the declining amplitude of voltage deflexions evoked by consecutive application of constant current pulses to cell 1 (1) and cell 2 (2). Towards the end of the experiment (right-hand side), there was no detectable voltage deflexion in the follower cell, suggesting functional uncoupling. $[K^+]_o$ = 4 mM; preparation M 79i.

Measurements of the resting potential varied considerably from one cell pair to another. Individual values typically ranged from −45 to −55 mV in the presence of 12 mM-K^+, and from −60 to −75 mV in the presence of 4 mM-K^+. As a general rule, resting potentials were more stable in the latter case (see also Powell *et al.* 1980).

Electrical stability of the cell pairs. When a cell pair was impaled with two micro-electrodes, stable recordings could be maintained for a minimum of 10–15 min. Thereafter, the cells began to depolarize gradually. Fig. 6 shows an example in which this terminal behaviour developed dramatically. As indicated in both panels, V_m of cell 1 and cell 2 depolarized slowly from −63 mV to −45 mV (phase *a*) and then suddenly to about −16 mV (phase *b*). The subsequent depolarization towards 0 mV again proceeded more slowly (phase *c*). Constant-current pulses (amplitude: 290 pA; duration: 200 ms) were applied consecutively to either cell at a frequency of 0·4 Hz, resulting in paired voltage deflexions in both cells. The results from this study showed that the cells were tightly coupled during phase *a* as indicated by the similar amplitude of electrotonic responses in cell 1 and cell 2. Analysis of such records at an expanded time scale yielded an R_m of 3770 Ω cm² and an r_n of 1·25 MΩ. During phase *b*, the cells remained coupled but the amplitude of the voltage deflexions

decreased. During phase *c* the injected current apparently was prevented from flowing across the nexal membrane, as indicated by the absence of a voltage deflexion in the follower cell. Because of the small size of the electrical responses, no reliable estimate of r_n was possible at this stage. Assuming complete uncoupling, R_m of cell 1 and cell 2 were 285 Ω cm² and 370 Ω cm², respectively. This type of triphasic behaviour was seen regularly during the course of our experiments. We never observed uncoupling with one of the cells remaining polarized and the other depolarized as reported by Kameyama (1983).

Single cells

Direct current (d.c.) also was employed to investigate the passive electrical properties of single ventricular myocytes. This enabled comparison with the electrical constants determined from cell pairs. The evoked membrane voltage was observed to change exponentially as a function of time. Therefore, it seemed justified to analyse the measurements in terms of a membrane resistance and a membrane capacitance in parallel. R_m was calculated from measurements of the input resistance ($R_{in} = dV/dI$) and cellular dimensions (a smooth circular cylinder was assumed). C_m was computed by dividing the membrane time constant (τ_m) by R_m ($C_m = \tau_m/R_m$). Individual measurements analysed in this fashion were collected by 10 mV intervals and plotted as histograms.

Fig. 7 summarizes the data obtained from ten different cells bathed in Krebs–Ringer solution containing 12 mM-K^+. It depicts the membrane potential dependence of the specific membrane resistance (R_m; continuous line histogram) and specific membrane capacity (C_m; dashed line histogram), respectively. Similar to the cell pairs (see Fig. 4*A*), the bell-shaped R_m function demonstrated a maximum (R_m = 12500 Ω cm²) at a V_m of −20 mV. At the most negative V_m explored, i.e. −60 mV, R_m averaged 1820 Ω cm². Statistical analysis uncovered a slight dependence of C_m on V_m (linear regression analysis: $2\alpha < 0{\cdot}01$; correlation coefficient $r = 0{\cdot}303$) with C_m increasing slightly as V_m became less negative. When all individual determinations were pooled, an average C_m of $1{\cdot}66 \pm 0{\cdot}05$ μF/cm² ($n = 81$) was calculated.

A similar set of experiments was performed on single cells exposed to Krebs–Ringer solution containing 4 mM-K^+. The collected data from twenty-nine myocytes are presented in Fig. 8, using the same format as in the previous Figure. Comparable to the findings made on cell pairs (see Fig. 5*A*), the R_m function showed a maximum (R_m = 10 720 Ω cm²) in the voltage range of −30 mV. At the most negative V_m investigated successfully, −80 mV, an R_m of 2570 Ω cm² was determined. Similar to the aforementioned statistical analysis demonstrated a barely significant correlation between C_m and V_m (linear regression analysis: $2\alpha < 0{\cdot}05$; correlation coefficient $r = 0{\cdot}163$). Averaging these C_m measurements yielded a mean value of $1{\cdot}61 \pm 0{\cdot}02$ μF/cm² ($n = 196$).

DISCUSSION

Sarcolemmal membrane

The resistance of the sarcolemmal membrane was determined from both single ventricular cells and cell pairs. In the first case R_m was extracted directly from the input resistance; in the second case R_m was obtained from the input resistance and

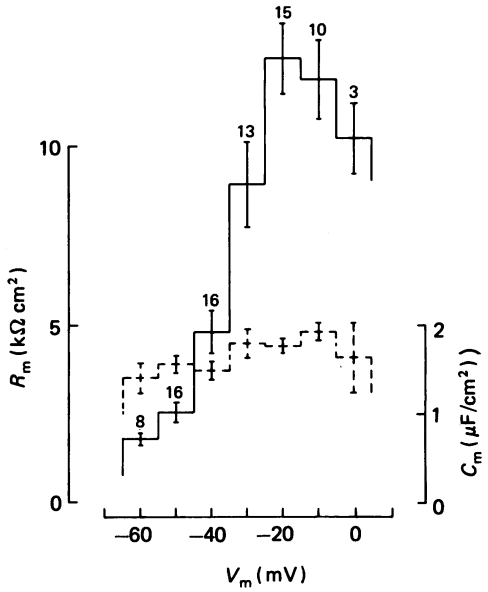

Fig. 7. Voltage dependence of passive electrical properties measured in single cells in the presence of 12 mM-K^+. The specific resistance of the sarcolemmal membrane, R_m (continuous line) and its specific capacitance, C_m (dashed line) were plotted as a function of the membrane potential, V_m. The bars represent the mean ± 1 S.E. of mean and the annotated figures signify the number of individual determinations. The data summarizes the results from ten cells.

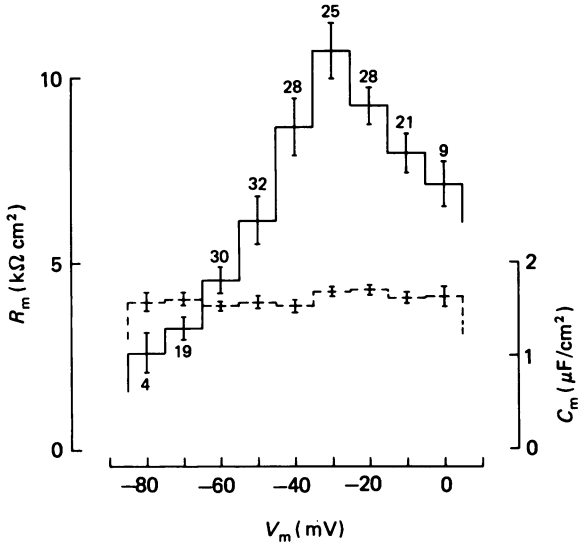

Fig. 8. Voltage dependence of passive electrical properties determined from single cells in the presence of 4 mM-K^+. Format and nomenclature are the same as in Fig. 7. The results from twenty-six individual cells are included.

the coupling coefficient by analysing the resistive elements of a simple network. Therefore, the comparison of the two data sets allowed a check for internal consistency. Furthermore, experiments were performed in the presence of either 12 or 4 mM-K^+. Here, the rationale was to search sources for possible systematic errors.

Both types of preparations, single cells and cell pairs, yielded bell-shaped relationships between R_m and V_m. This held true whether the experiments were performed in Tyrode solution containing 12 mM-K^+ (compare Figs. 4*A* and 7) or 4 mM-K^+ (compare Figs. 5*A* and 8). The measured resistance functions resemble those previously reported by Powell *et al.* (1980) on the same preparation. The steady-state current–voltage relationship obtained from intact mammalian ventricular preparations (e.g. Trautwein & McDonald, 1978) or dispersed ventricular cells (Isenberg & Klöckner, 1982*b*; Sakmann & Trube, 1984) predicts the following changes upon lowering $[K^+]_o$ from 12 to 4 mM: (1) a shift of the resistance function along the voltage axis towards more negative values; (2) an increase of the amplitude of the resistance function along its entire extent. Our observations are in agreement with the first prediction in that lowering of $[K^+]_o$ led to a shift of the R_m/V_m relationship in the expected direction by approximately 10 mV (compare Figs. 4*A* and 5*A*, and 7 and 8, respectively). The second prediction was fulfilled over the range of more negative potentials, but not near the potential where the resistance function reached a peak. There are several reasons why we may have failed to detect the latter. One possibility is that our input resistance determinations were impaired by a considerable shunt resistance arising from a leak around the electrode tip. The possibility of such a shunt would be increased whenever the input resistance increased – a setting existing in the potential range near the peak of the R_m/V_m relationship. Another possibility may be that the electrode shunt resistance decreased in 4 mM-K^+ solution for some unknown reason. Furthermore, one must remember that the 'slope resistance' determinations are relatively inaccurate over the potential range -30 to -10 mV because large voltage deflexions are elicited by relatively small currents. In fact, no reliable measurements could be obtained over this voltage range in some cells because of the negative slope of the current–voltage relationship (see, e.g. Trautwein & McDonald, 1978).

The question now arises as to what the real value of R_m is for cardiac muscle cells at their resting membrane potential. The following values were deduced from our own experiments on dispersed rat ventricular cells. Single cells: $R_m = 2{\cdot}5$ kΩ cm² ($[K^+]_o = 12$ mM; Fig. 7) and 3·25 kΩ cm² ($[K^+]_o = 4$ mM; Fig. 8); cell pairs: $R_m = 3{\cdot}2$ kΩ cm² ($[K^+]_o = 12$ mM; Fig. 4) and 4·3 kΩ cm² ($[K^+]_o = 4$ mM; Fig. 5). Individual values of V_m ranged from -45 to -55 mV ($[K^+]_o = 12$ mM), and from -60 to -75 mV ($[K^+]_o = 4$ mM), respectively. These values of R_m are comparable to those previously reported for isolated adult heart cells from mammals (Powell *et al.* (1980): $R_m = 2{\cdot}4$ kΩ cm², $[K^+]_o = 3{\cdot}8$ mM; Brown, Lee & Powell, (1981): $R_m = 2{\cdot}8$ kΩ cm², $[K^+]_o = 4{\cdot}8$ mM; Isenberg & Klöckner (1982*a*): $R_m = 6{\cdot}9$ kΩ cm², $[K^+]_o = 5{\cdot}4$ mM) and neonatal rat heart cells (Hyde, Blondel, Matter, Cheneval, Filloux & Girardier (1969): $R_m = 5{\cdot}5$ kΩ cm², $[K^+]_o = 5{\cdot}4$ mM; Jongsma & van Rijn (1972): $R_m = 1{\cdot}3$–$2{\cdot}6$ kΩ cm², $[K^+]_o = 4{\cdot}7$ mM). However, any one of these values is slightly lower than the one reported for intact mammalian trabeculae (Weidmann, 1970): $R_m = 9{\cdot}1$ kΩ cm², $[K^+]_o = 5{\cdot}4$ mM). A likely reason for this discrepancy may

lie within differences in the assumed morphology (see below) rather than in the experimental approach.

The single-cell experiments enabled us to determine the capacity of the sarcolemmal membrane as well. The measurements yielded slightly larger values of C_m at less negative membrane potentials. However, this dependency of C_m on V_m was only barely significant for both experimental conditions, i.e. $[K^+]_o = 12$ and 4 mM. It is conceivable that this observation reflects the difficulty in taking exact measurements of τ_m at lower values of R_m. Further experiments are needed to clarify this question. Pooling the individual determinations, the specific capacity was found to be 1·66 μF/cm^2 ($[K^+]_o = 12$ mM) and 1·61 μF/cm^2 ($[K^+]_o = 4$ mM), respectively. The two means do not differ significantly from each other (Student's t test: $P > 0{\cdot}1$). This finding agrees with the view that the capacitance of biomembranes is markably stable even under conditions of large physiological change (Cole, 1968). Our values of C_m are slightly lower than those previously reported for the same type of cellular preparation (Powell *et al.* (1980): 2·5 μF/cm^2; Brown *et al.* (1981): 5·0 μF/cm^2), but slightly larger than those obtained from multicellular preparations (Weidmann (1970): 0·81 μF/cm^2, mammalian ventricle; Jongsma & van Rijn (1972): 0·7–1·3 μF/cm^2, cultivated neonatal rat heart cells). If one assumes a specific membrane capacity of 1 μF/cm^2, the surface membrane area used in our calculations would have been too low by 61–66 %. Hence, the values of R_m reported above would be underestimated by the same factor.

There are several reasons as to why the adopted myocyte surface area may be erroneous. First of all, the assumption of a cylindrical geometry must have been a gross simplification in view of the irregular nature of the cellular shapes (see, e.g. Sommer & Johnson, 1979). More important, however, the total surface area of a cardiac cell not only consists of the external sarcolemmal membrane with its foldings, it also involves the T-tubular membrane (Stewart & Page, 1978) and presumably the caveolar surface membrane (Gabella, 1978). Based on stereological analysis performed on rat ventricular tissue (Stewart & Page, 1978), an average cell has a length of 102 μm and a diameter of 13·3 μm. Such an idealized cell has a cellular volume of 14200 μm^3 and a total surface membrane area of 7575 μm^2 (external sarcolemma: 4350 μm^2; T-tubular membrane: 2050 μm^2; caveolar surface membrane: 1175 μm^2; Stewart & Page, 1978; Gabella, 1978). Without doubt, these values are more accurate than those based on light-microscopic observations of single cells *in vitro*. However, since these results were obtained from tissues processed for electron microscopy, they may not be readily transferred to more physiological conditions. Our own series of measurements carried out on living rat ventricular myocytes revealed a cell length of 111·5 $\pm$ 2·1 μm and a cell diameter of 19·9 $\pm$ 0·5 μm ($n = 59$; R. Weingart, unpublished observation), yielding a cell volume of 34700 μm^3 and a cylindrical surface area of 7600 μm^2. These cell dimensions are close to those previously reported by Korecky & Rakusan (1978; length: 119·9 μm; diameter: 22·2 μm) and Krueger, Forletti & Wittenberg (1980; length: 115 μm; diameter: 22 μm). This means that the total surface area obtained from the stereological analysis barely provides a *cylindrical* envelope for a living myocyte. This discrepancy suggests that severe volume changes must occur during the treatment of the tissues for electron microscopy. Referring to the cell dimensions given by Stewart & Page (1978), the volume shrinkage may be

as much as 60 %. In fact, similar shrinkage factors have been reported previously by Eisenberg & Mobley (1975) for skeletal muscle and by Rostgaard & Tranum-Jensen (1980) for gall-bladder. From this we conclude that serious problems may arise when attempting to correlate ultrastructural with functional parameters unless volume shrinkage is considered. Unfortunately, a systematic study focussing on this problem is unavailable for cardiac tissue at the present time.

Nexal membrane

As discussed above, R_m values were measured in single cells which were comparable to those determined in multicellular tissues. This implies that the sarcolemmal membrane was not shunted by another low resistance membrane. Hence, the disruption of a cell from its neighbours did not result in a significant current leak at the former points of attachment. This suggests that the low resistance junctional membranes must have sealed during the isolation procedure. One possibility is that dispersion of adjacent cells occurred in such a manner that one cell became void of nexal membrane while the other one retained the intact junctional membrane, protected by a membrane vesicle (Severs, Slade, Powell, Twist & Warren, 1982). Alternatively, the nexal membrane of a single cell may have closed up its channels such as has been suggested for 'healing over' (see, e.g. De Mello, 1982).

Data concerning the electrical properties of the nexal membrane was obtained from measurements on cell pairs. The cell pairs employed presumably represent incompletely disintegrated tissue rather than cells recoupled *in vitro*. This seems likely because cell pairs were already observable during early stages of the isolation procedure, i.e. during the incubation of the tissue slices. Furthermore, all experiments were performed within 6 h after isolation, a period of time which is too short in order to establish spontaneous recoupling (see, e.g. Hyde *et al.* 1969; Jongsma & van Rijn, 1972). The isolation procedure yielded cell pairs in a side-to-side configuration having a variable degree of overlap (see Pl. 1 *B*) together with cell pairs arranged end-to-end. Because of their rarity, the latter were not used in this study. There may be several reasons for the dissimilar occurrence of the two types of preparation. (1) It is well-known that cell boundaries are usually staggered at the intercalated disks (see, e.g., Sommer & Johnson, 1979). This geometry *per se* may underlie the common appearance of the side-to-side configuration. (2) Preparations of the end-to-end configuration are likely to be less stable mechanically in a stirred cell suspension.

A qualitative hint for the existence of functional coupling between the cells of an isolated cell pair came from investigating the intrinsic electrical cell activity (see Fig. 2). We have obtained direct evidence from cell pairs at negative values of V_m ($V_m > -60$ mV) as well as in partially depolarized preparations ($V_m \cong -40$ mV).

More quantitative information about the electrical properties of the nexal membrane was obtained from current-clamp experiments. These studies revealed no evidence for the existence of a correlation between nexal membrane resistance and the potential across the sarcolemmal membrane over the potential range from -70 to -10 mV (see Figs. 4 *B* and 5 *B*). This finding concurs with recent reports from guinea-pig and rat ventricular cell pairs (Kameyama, 1983; White, Spray, Schwartz, Wittenberg & Bennett, 1984). The lack of voltage dependence seems to suggest that the nexal conductance is insensitive to voltage gradients between the sarcoplasm and

the extracellular fluid. In addition, this finding may indicate that the elevation in $[Ca^{2+}]_i$ associated with depolarization towards -10 mV may not be sufficient to alter the nexal conductance measurably. This conclusion is in line with an earlier observation obtained on ventricular multicellular preparation. Weidmann (1970) reported that, during an action potential, a putative impairment of electrical coupling between cardiac cells must be rather small, if present at all.

Our experiments on cell pairs revealed no sign of a difference in junctional resistance whether current was injected into cell 1 or cell 2. This suggests that current spreads across the junctional membrane equally well in both directions. This observation seems to exclude an asymmetric nature of the junctional membrane properties as a possible explanation for uni-directional slowing of the conduction velocity in heart (see, e.g. Mendez, Mueller & Urquiaga, 1970; Veenstra, Joyner & Rawling, 1984). Therefore, the nexal membrane of cardiac cells resembles the junctional membrane in amphibian embryos (Spray, Harris & Bennett, 1981) in that both lack a V_m-dependent conductance and a rectifier. In contrast, the junctional membrane of *Chironomus* salivary glands was reported to possess a sigmoidal dependence of its conductance on V_m (Obaid, Socolar & Rose, 1983; but see also Metzger & Weingart, 1984). Or, the gap junction of the giant motor synapse of crayfish was found to enable uni-directional transmission of electrical signals only (Furshpan & Potter, 1959).

For comparison, we have carried out current-clamp experiments on cell pairs immersed in Krebs–Ringer solution of different $[K^+]$. The analysis revealed numerical values of r_n which did not differ significantly from each other, whether the bathing $[K^+]_o$ was 4 or 12 mM ($r_n = 2{\cdot}27$ MΩ and $2{\cdot}12$ MΩ, respectively; Student's t test: $P > 0{\cdot}3$). This finding also lends support to the above conclusion that the nexal resistance does not depend on V_m. Our values of r_n are in good agreement with those reported by Kameyama (1983) for guinea-pig ventricular cell pairs ($[K^+]_o = 5{\cdot}4$ mM: $r_n = 2{\cdot}1$ MΩ; $[K^+]_o = 10{\cdot}8$ mM: $r_n = 1{\cdot}4$ MΩ). However, our values of r_n are much lower than those reported by White *et al.* (1984) for rat ventricular cell pairs ($r_n = 10$–200 MΩ). A possible explanation for this discrepancy may be that White *et al.* (1984) investigated nexal membranes of re-established cell pairs, while we (and Kameyama, 1983) dealt with cell pairs from incompletely disintegrated tissue (see p. 191).

R_n then was determined from r_n and the nexal membrane area gleaned from stereological studies (Stewart & Page, 1978). The following values were calculated: $[K^+]_o = 12$ mM: $R_n = 0{\cdot}10$ Ω cm²; $[K^+]_o = 4$ mM: $R_n = 0{\cdot}12$ Ω cm². It would be interesting to compare these numbers with those gained from the work performed on multicellular cardiac preparations by means of the conventional cable analysis. Our own analysis on cell pairs assumed that the cytoplasmic resistance r_c can be lumped together with the nexal membrane resistance r_n (see p. 181). Therefore, a meaningful comparison requires a similar treatment of the results obtained from the intact tissues as well. Experiments performed on monolayers of neonatal rat heart cells have found the intracellular longitudinal resistance R_i to be 540 Ω cm (Hyde *et al.* 1969) and 500 Ω cm (Jongsma & van Rijn, 1972). The latter group reported an R_m ranging from $0{\cdot}33$ to $1{\cdot}65$ Ω cm² under the above assumption. Weidmann (1970), who studied intact calf ventricular muscle, determined an R_i of 470 Ω cm. Using an

interdisk distance $h = 100\ \mu m$, and a ratio nexal membrane area/cross-section area $g = 0{\cdot}24$ (Stewart & Page, 1978), R_n turns out to be $1{\cdot}13\ \Omega\ cm^2$ ($R_n = R_i\, h\, g$). This suggests that the R_n values extracted from studies of multicellular mammalian tissues are generally larger, in the latter case by as much as 10-fold. However, facing this discrepancy, it is presumably fair to state that the prime weakness of such comparisons is related to the incomplete anatomical data available rather than differences in experimental approaches. With regard to this problem, progress was recently made in case of amphibian heart tissue. Haas, Meyer, Einwächter & Stockem (1983) carried out studies on frog ventricular muscle focussing on both electrophysiological and morphological aspects of intracellular coupling. On the assumption that r_c may be ignored, their data revealed an R_n of $0{\cdot}77\ \Omega\ cm^2$. However, there seem to be pronounced morphological differences of the nexal membrane in mammalian and amphibian cardiac tissues (for references, see Sommer & Johnson, 1979; Haas *et al.* 1983). Therefore, it is conceivable that there exist functional differences among these species as well.

Cell pairs isolated from intact hearts by means of enzymatic procedures represent a simple preparation highly suitable for studying the electrical properties of the nexal membrane. In a first attempt we have used the current-clamp technique in conjunction with a balanced-bridge circuit and conventional micro-electrodes. This approach, although it has inherent limitations, enabled quantitative information to be obtained about the fundamental electrical properties of the junctional membrane of cardiac tissue. However, in order to gain further insight into the molecular basis of the mechanism(s) which control the intercellular coupling, more advanced techniques will need to be applied to such preparations in the future.

We are grateful to Miss M. Herrenschwand, Messrs. C. Cigada and A. Meyer for their expert technical assistance and to Dr M. L. Pressler for critical comments on the manuscript. This research was supported by the Swiss National Science Foundation (3.565-0.79 and 3.360-0.82) and the Swiss Foundation of Cardiology.

REFERENCES

BENNETT, M. V. L. (1966). Physiology of electrotonic junctions. *Annals of the New York Academy of Sciences* **137**, 509–539.

BERKENBLIT, M. B., BOSCHKOVA, W. P., BOJZOWA, L. J., MITTELMAN, L. A., POTAPOWA, T. W., TSCHAJLACHJAN, L. M. & SCHAROWSKAJA, J. J. (1981). In *High Conductance Junctional Membranes* (In Russian), p. 48. Moscow: Nauka.

BROWN, A. M., LEE, K. S. & POWELL, T. (1981). Voltage clamp and internal perfusion of single rat heart muscle cells. *Journal of Physiology* **318**, 455–477.

COLE, K. C. (1968). In *Membranes, Ions and Impulses*. Berkeley: University of California Press.

DE MELLO, W. C. (1982). Cell-to-cell communication in heart and other tissues. *Progress in Biophysics and Molecular Biology* **39**, 147–182.

EISENBERG, R. S. & JOHNSON, E. A. (1970). Three-dimensional electrical field problems in physiology. *Progress in Biophysics and Molecular Biology* **20**, 1–65.

EISENBERG, B. R. & MOBLEY, B. A. (1975). Size changes in single muscle fibers during fixation and embedding. *Tissue and Cell* **7**, 383–387.

EISENBERG, B. R. & COHEN, I. S. (1983). The ultrastructure of the cardiac Purkinje strand in the dog: a morphometric analysis. *Proceedings of the Royal Society* B **217**, 191–213.

FABIATO, A. (1981). Myoplasmic free calcium concentration reached during the twitch of an intact isolated cardiac cell and during calcium-induced release of calcium from the sarcoplasmic

reticulum of a skinned cardiac cell from the adult rat or rabbit ventricle. *Journal of General Physiology* **78**, 457–497.

FOZZARD, H. A. (1979). Conduction of the action potential. In *Handbook of Physiology* **1**, sect. 2, *Cardiovascular System*, pp. 335–356. Washington: American Physiological Society.

FURSHPAN, E. J. & POTTER, D. D. (1959). Transmission at the giant motor synapses of the crayfish. *Journal of Physiology* **145**, 289–325.

GABELLA, G. (1978). Inpocketings of the cell membrane (caveolae) in the rat myocardium. *Journal of Ultrastructural Research* **65**, 135–147.

HAAS, H. G., MEYER, R., EINWÄCHTER, H. M. & STOCKEM, W. (1983). Intercellular coupling in frog heart muscle. Electrophysiological and morphological aspects. *Pflügers Archiv* **399**, 321–335.

HESS, P., METZGER, P. & WEINGART, R. (1982). Free magnesium in sheep, ferret and frog striated muscle at rest measured with ion-selective micro-electrodes. *Journal of Physiology* **333**, 173–188.

HODGKIN, A. L. & RUSHTON, W. A. H. (1946). The electrical constants of a crustacean nerve fibre. *Proceedings of the Royal Society* B **133**, 444–479.

HYDE, A., BLONDEL, B., MATTER, A., CHENEVAL, J. P., FILLOUX, B. & GIRARDIER, L. (1969). Homo- and heterocellular junctions in cell cultures: an electrophysiological and morphological study. In *Progress in Brain Research*, vol. **31**, ed. AKERT, K. & WASER, P. G., pp. 283–311. Amsterdam: Elsevier.

ISENBERG, G. & KLÖCKNER, U. (1982*a*). Calcium tolerant ventricular myocytes prepared by preincubation in a 'KB medium'. *Pflügers Archiv* **395**, 6–18.

ISENBERG, G. & KLÖCKNER, U. (1982*b*). Isolated bovine ventricular myocytes. Characterization of the action potential. *Pflügers Archiv* **395**, 19–29.

JONGSMA, H. J. & VAN RIJN, H. E. (1972). Electrotonic spread of current in monolayer cultures of neonatal rat heart cells. *Journal of Membrane Biology* **9**, 341–360.

KAMEYAMA, M. (1983). Electrical coupling between ventricular paired cells isolated from guinea-pig heart. *Journal of Physiology* **336**, 345–357.

KORECKY, B. & RAKUSAN, K. (1978). Normal and hypertrophic growth of the rat heart: changes in cell dimensions and number. *American Journal of Physiology* **234**, H123–128.

KRUEGER, J. W., FORLETTI, D. & WITTENBERG, B. A. (1980). Uniform sarcomere shortening behaviour in isolated cardiac muscle cells. *Journal of General Physiology* **76**, 587–607.

LEVIS, R. A., MATHIAS, R. T. & EISENBERG, R. S. (1983). Electrical properties of sheep Purkinje strands. Electrical and chemical potentials in the clefts. *Biophysical Journal* **44**, 225–248.

MATHIAS, R. T. (1983). Effect of tortuous extracellular pathways on resistance measurements. *Biophysical Journal* **42**, 55–59.

MENDEZ, C., MUELLER, W. J. & URQUIAGA, X. (1970). Propagation of impulses across the Purkinje fiber–muscle junctions in the dog heart. *Circulation* **26**, 135–150.

METZGER, P. & WEINGART, R. (1983). Electrical coupling of cell pairs isolated from adult rat hearts. *Journal of Physiology* **336**, 67–68*P*.

METZGER, P. & WEINGART, R. (1984). Electric current flow in a two-cell preparation from chironomus salivary glands. *Journal of Physiology* **346**, 599–619.

OBAID, A. L., SOCOLAR, S. L. & ROSE, B. (1983). Cell-to-cell channels with two independently regulated gates in series: analysis of junctional conductance modulation by membrane potential, calcium and pH. *Journal of Membrane Biology* **73**, 69–89.

POWELL, T., TERRAR, D. A. & TWIST, V. W. (1980). Electrical properties of individual cells isolated from adult rat ventricular myocardium. *Journal of Physiology* **302**, 131–153.

PRESSLER, M., (1984). Cable analysis in quiescent and active sheep Purkinje fibres. *Journal of Physiology* **352**, 739–757.

ROSTGAARD, J., TRANUM-JENSEN, J. (1980). A procedure for minimizing cellular shrinkage in electron microscope preparation: a quantitative study on frog gall bladder. *Journal of Microscopy* **119**, 213–232.

SAKMANN, B. & TRUBE, G. (1984). Conductance properties of single inwardly rectifying potassium channels in ventricular cells from guinea-pig heart. *Journal of Physiology* **347**, 641–657.

SEVERS, N. J., SLADE, A. M., POWELL, T., TWIST, V. M. & WARREN, R. L. (1982). Correlation of ultrastructure and function in calcium-tolerant myocytes isolated from the adult rat heart. *Journal of Ultrastructural Research* **81**, 222–239.

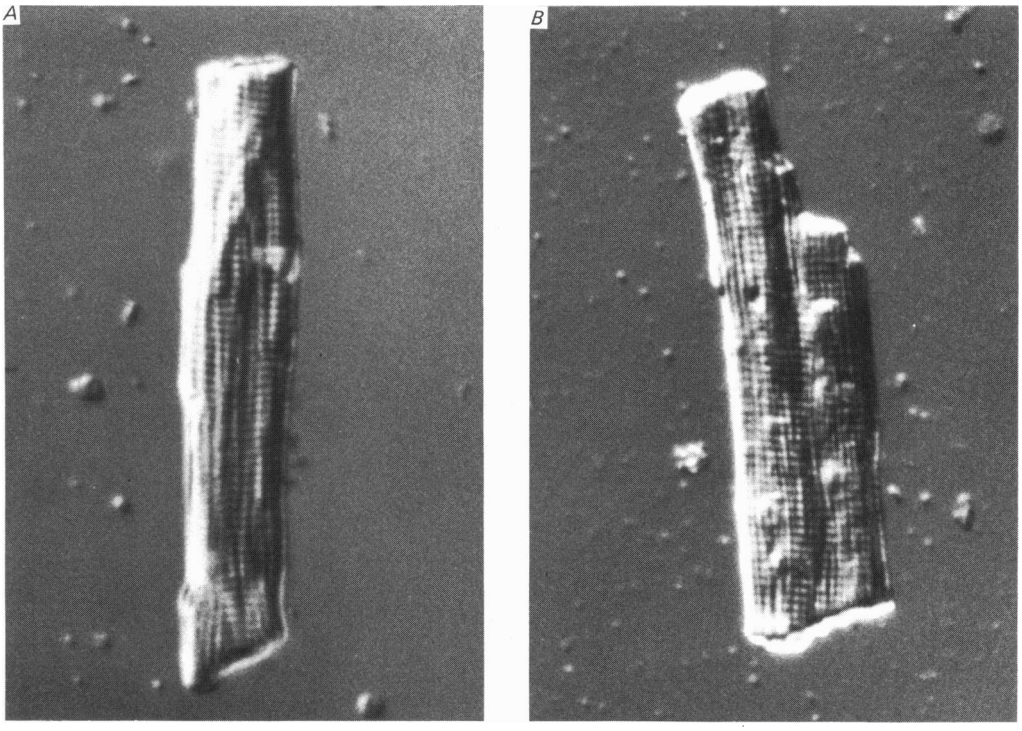
A
B

SOMMER, J. R. & JOHNSON, E. A. (1979). Ultrastructure of cardiac muscle. In *Handbook of Physiology*, sect. 2, *The Cardiovascular System*, vol. I, *The Heart*, ed. BERNE, R. M., pp. 113–186. Washington: American Physiological Society.

SPRAY, D. C., HARRIS, A. L. & BENNETT, M. V. L. (1981). Equilibrium properties of a voltage-dependent junctional conductance. *Journal of General Physiology* **77**, 77–93.

STEWART, J. M. & PAGE, E. (1978). Improved stereological techniques for studying myocardial cell growth: application to external sarcolemma, T-system, and intercalated disks of rabbit and rat hearts. *Journal of Ultrastructural Research* **65**, 119–134.

TRAUTWEIN, W. & MCDONALD, T. F. (1978). Current–voltage relations in ventricular muscle preparations from different species. *Pflügers Archiv* **374**, 79–89.

TSIEN, R. W, KASS, R. S. & WEINGART, R. (1979). Cellular and subcellular mechanisms of cardiac pacemaker oscillations. *Journal of Experimental Biology* **81**, 205–215.

VEENSTRA, R. D., JOYNER, R. W. & RAWLING, D. A. (1984). Purkinje and ventricular activation sequences of canine papillary muscle. *Circulation Research* **54**, 500–515.

WATANABE, A. & GRUNDFEST, H. (1961). Impulse propagation at the septal and commissural junctions of crayfish lateral giant axons. *Journal of General Physiology* **45**, 267–308.

WIEDMANN, S. (1952). The electrical constants of Purkinje fibres. *Journal of Physiology* **118**, 348–360.

WIEDMANN, S. (1970). Electrical constants of trabecular muscle from mammalian heart. *Journal of Physiology* **210**, 1041–1054.

WEINGART, R. (1981). Cell-to-cell coupling in cardiac tissue. In *Advanced Physiological Science* **8**, ed. KOVACH, A. G. B., MONOS, E. & RUBANYI, G., pp. 59–68. New York: Pergamon Press.

WHITE, R. L., SPRAY, D. C., SCHWARTZ, G. J., WITTENBERG, B. A. & BENNETT, M. V. L. (1984). Some physiological and pharmacological properties of cardiac gap junctions. *Biophysical Journal* **45**, 279a.

EXPLANATION OF PLATE

Interference contrast photomicrographs (Nomarski optics with water immersion) of isolated rat myocytes showing regular striation patterns. *A*, rod-shaped single ventricular cell (length = 130 μm, diameter = 18 μm). *B*, cell pair oriented side-to-side. Primarily this type of cell configuration was used to study the nexal membrane properties. Picture courtesy of Professor Ewald Weibel, Department of Anatomy, University of Berne.